Rapid Analysis of the Size Distribution of Metal-Containing Aerosol

Jae Hong Park[1], **Imali A. Mudunkotuwa**[2], **Kathryn J. Crawford**[3], **T. Renée Anthony**[3], **Vicki H. Grassian**[4], and **Thomas M. Peters**[3,*]

[1]School of Health Sciences, Purdue University, Indiana

[2]Department of Chemistry, University of Iowa, Iowa

[3]Department of Occupational and Environmental Health, University of Iowa, Iowa

[4]Departments of Chemistry and Biochemistry and Nanoengineering, University of California San Diego, California

Abstract

Conventional methods to measure the metallic content of particles by size are time consuming and expensive, requiring collection of particles with a cascade impactor and subsequent metals analysis by inductively coupled plasma mass spectrometry (ICP-MS). In this work, we describe a rapid way to measure the size distribution of metal-containing particles from 10 nm to 20 μm, using a nano micro-orifice uniform-deposit impactor (nano-MOUDI) to size-selective and collect particles that are then analyzed with a field portable X-ray fluorescence (FP-XRF) to determine metal composition and concentration. The nano-MOUDI was used to sample a stainless-steel aerosol produced by a spark discharge system. The particle-laden substrates were then analyzed directly with FP-XRF and then with ICP-MS. Results from FP-XRF were linearly correlated with results from ICP-MS ($R^2 = 0.91$ for Fe and $R^2 = 0.84$ for Cr). Although the FP-XRF was unable to detect Fe particles at mass per substrate loadings less than 2.5 μg effectively, it produced results similar to those using the ICP-MS at a mass per substrate loading greater than 2.5 μg.

Keywords

nano-MOUDI; X-ray fluorescence; inductively coupled plasma; stainless-steel aerosol; mass spectrometry

1. Introduction

Measurements of the particle size distribution of the different components of metal-containing aerosols are important for a wide range of applications from evaluating health risks from exposures to optimizing industrial production. Such size distributions can be measured in situ or through collection on a substrate by particle samplers for further analysis. Aerosol time of flight mass spectrometers (ATOFMS) can be used to characterize

*Corresponding author: Thomas M. Peters, PhD, 105 River St, S331 CPHB, University of Iowa, Iowa City, Iowa 52242, Thomas-m-peters@uiowa.edu.

the chemical speciation of metals in situ (Hughes et al., 1999). However they are sometimes impractical for field study because they are expensive (> $500,000) and large ($1.7 \times 0.74 \times 1.3$ m^3). Cascade impactors can be used to collect particles by size on collection substrates (Hering et al., 1997). The metallic content of these collected particles can then be determined using various methods of off line measurements.

A micro-orifice uniform deposition impactor (MOUDI) (MSP Corp., Shoreview, MN, USA; Marple et al., 1991) is one of the most commonly used commercial devices for sampling and size-resolving fine particles including nanoparticles (Chow and Watson 2007). A nano-MOUDI (model 125-R, MSP, Shoreview, MN, USA) is a 13-stage cascade impactor that allows the separation of particles into 13 size classes ranging from 10 nm to 10 μm (cut-off diameters are 0.010, 0.018, 0.032, 0.056, 0.10, 0.18, 0.32, 0.56, 1.0, 1.8, 3.2, 5.6, and 10 μm). A backup filter is located at the end of the series in the final stage and collects particles smaller than 10 nm. The nano-MOUDI is considered to be a second-generation MOUDI. Changes from the first model include the addition of internal motors in each stage that rotate the impaction plates to help to reduce particle bounce and thus decreases the chance of improperly sized particles. The rotation also helps uniform deposition of particles on the plate which helps decrease overloading (Marple et al., 2014). A second improvement to the second generation MOUDI is the reduction of obstacles in the flow path between the impaction and nozzle plates, which should reduce internal losses to diffusion (Marple et al., 2014). The nano-MOUDI is commercially available with aluminum (Al) alloy impaction plates (substrate holder) and is typically operated with Al substrates. The company recommends using substrates thinner than 100 μm.

Inductively coupled plasma (ICP)-based mass and optical measurement techniques are typically used to quantify the metal content of particles collected on impaction substrates. The substrates with particles need to be washed or dissolved with a mixture of acids before analysis by ICP-optical emission spectrometry (OES), -atomic emission spectrometry (AES) or mass spectrometry (MS) (Herner et al., 2006). These methods allow measurements of specific metals at low concentrations (ppm ~ ppt). Broekaert (1982) used an ICP-OES to analyze metals in aerosol samples collected with a cascade impactor. Espinosa et al. (2001; 2002) used an ICP-AES to measure the size distribution of metals in an urban atmosphere. Onat et al. (2012) used an ICP-MS to measure the size distribution of heavy metals in urban airborne particles. However, ICP-based techniques are often time consuming and can also be costly. This method also results in sample destruction limiting further analysis.

Another method of analysis is X-ray fluorescence spectroscopy (XRF). The XRF method yields less sensitivity replicate measurements than ICP-based techniques, but is not destructive, relatively easy to operate, and provides simultaneous multi-elemental information. There are different kinds of XRF methods. For example, Cuccia et al. (2013) used an energy dispersive-XRF (ED-XRF) while Achad et al. (2014) and Bukowiecki et al. (2005) used a synchrotron radiation-XRF (SR-XRF) to determine elemental composition of urban airborne particles sampled with impactors. However, benchtop XRF instruments are still impractical for field use because they are not portable.

More recently, field portable-XRFs (FP-XRFs) have been developed. These are fully portable, hand-held instruments that enable rapid, cost effective measurement of metal content in samples with little sample preparation. Ashley (2010) provided an overview of FP-XRFs to determine a wide range of metals in sampled particles on the air filters or wipes. In several studies, researchers have used FP-XRFs to measure occupational exposures to metals (Laohaudomchok et al., 2010; Gorce and Roff, 2016; Harper et al., 2007). However, these studies measure only total concentrations since particles were collected using air filters without size classification. The National Institute for Occupational Safety and Health (NIOSH) developed a standard analytical method (Method 7702) for determining the concentration of lead in particles collected by air filters using FP-XRF technology (NIOSH, 1998). To our knowledge, no study to date has used both a cascade impactor and FP-XRF to determine the size distribution of metals in airborne particles.

In this paper, we present a rapid way to assess the size distribution and the metal content of airborne particles using a nano-MOUDI for particle collection and a FP-XRF for metals analysis. In order to reduce interference from the substrate holders during FP-XRF metals analysis, custom polyether ether ketone (PEEK) substrate holders were made and polycarbonate (PC) substrates were used for collection with the nano-MOUDI. We collected stainless steel particles and analyzed their iron (Fe) and chromium (Cr) content. We validate these results in a laboratory study using the more established method of ICP-MS. As an example application, we then apply this method and the data obtained in our tests to estimate occupational exposure (inhalable, thoracic, and respirable) and dose (nose and head, tracheobronchial, thoracic, and alveolar regions).

2. Materials and Methods

2.1. Development of a method to use FP-XRF with the nano-MOUDI

First, we investigated the influence of substrate holder material on measurements by FP-XRF. The substrate holders supplied with the nano-MOUDI are composed of Al alloy with a magnet attached to the backside. Holders with the same dimensions as the supplied Al holders were machined from polyether ether ketone (PEEK). The PEEK holders were not fitted with a magnet on the backside. (Figure 1(a)).

The Al alloy and PEEK holders were analyzed by FP-XRF (Niton XL3t Ultra, Thermo Scientific, USA) with and without substrates (for each holder material, n = 3 without substrate and n = 9 with substrate, total 24 measurements). For substrates, PC filters (PCT0247100, pore size of 0.2 μm, diameter of 47 mm, Sterlitech, USA) were coated with silicone oil (Heavy-duty silicone spray, Part #07041, MSP Corp., Shoreview, MN, USA) to prevent particle bounce. The oil was applied using a foam stamp (diameter of 20 mm; see supplemental information) and then placed in an oven at 50°C for five hours to evaporate volatile components in the oil. We selected this substrate because it can be fully digested with a microwave-assisted acid digestion method as specified below. A 3D-printed support (see supplemental information) was used to keep a consistent distance between the FP-XRF and the surface of holder, to ensure consistency between analyses. The FP-XRF thin-film (standard filter) mode was used to measure metals in units of μg/cm^2. The measurement time

was set to 120 seconds (main range: 40 seconds, low range: 40 seconds, and high range: 40 seconds).

2.2. Comparison of size distribution measurements analyzed by FP-XRF to ICP-MS

The experimental setup is shown schematically in Figure 1(b). Dry and particle-free air, controlled by a mass flow controller (MFC; MPC20, Porter Instrument, USA), was delivered to a spark discharge system equipped with stainless steel electrodes (303 alloy; 2EXC7, Grainger, USA) to generate stainless steel particles (Park et al., 2015). Highly charged, <10 nm sized, and chain-like aggregated particles containing Cr and Fe, were generated from the spark discharge system. The test particles were passed through a polonium-210 aerosol neutralizer (2U500, Staticmaster, USA) to neutralize their charge to Boltzmann equilibrium, then passed through a coagulation chamber (200 L) to increase their size from <10 nm to larger than 60 nm, and finally delivered to a sampling chamber (22 L). The concentration of test particles was diluted by room air that was first passed through a high efficiency particulate air (HEPA) filter. An MFC and vacuum pump were used to control the airflow rate of dilution air.

The test particles were sampled using a nano-MOUDI (Model 125-R, MSP, USA) at an airflow rate of 10 L/min. Polycarbonate substrates were fixed to the PEEK holders and loaded into the nano-MOUDI stages for particle collection. A mixed cellulose ester (MCE) filter (FMCE847, pore size of 0.8 μm, diameter of 47 mm, Zefon International, Inc., FL, USA) was used as a backup filter. The sampling time was four hours (sampling volume of 2.4 m^3) and sampling was performed in triplicate.

The particle-laden substrates were analyzed directly using a FP-XRF (Niton XL3t Ultra, Thermo Scientific, USA) as shown in Figure 1(a). After analyzing Fe and Cr content, and the mass per substrate of i-th stage (M_i) of nano-MOUDI was calculated as follows:

$$M_i = (M_{Ai} - M_{Ab}) \times A_i \quad (1)$$

where M_{Ai} and M_{Ab} are the mass per unit area of i-th stage and blank substrates, respectively. To account for possible variations in the mass of the blank substrates in the calculations, the average value of nine black substrates was used for M_{Ab}. A_i is the sampled area of the nano-MOUDI at the i-th stage ($A_{1,3-10} = 1.8$ cm^2, $A_{2,11} = 3.1$ cm^2, $A_{12} = 4.9$ cm^2, $A_{13} = 5.7$ cm^2, and $A_{14} = 10.8$ cm^2).

Following the FP-XRF analysis, the particle-laden substrates were subjected to microwave-assisted acid digestion. The digestion protocol was a slightly modified version of the protocol used to dissolve TiO_2 nanoparticles in our previous study (Mudunkotuwa et al., 2016). Briefly, the particle laden substrates were carefully placed in Teflon digestion vessels, a combination of conc. H_2SO_4 (6 mL) and conc. HNO_3 (3 mL) was added, and the substrates were digested using a microwave digestion system (MARS 6, CEM Corporation, USA) for 45 minutes. The digestate was added to vials containing water (10 mL) and allowed to degas overnight in the fume hood. An additional dilution step (10 times dilution)

was carried out to reduce the acidity of the medium. Finally, the solutions were topped up to 30 mL with water and analyzed by ICP-MS. The Fe and Cr content was analyzed and the values for mass per substrate were blank-subtracted.

For each metal, the mass per substrate measured by FP-XRF and ICP-MS were converted to mass concentration (C_i) as:

$$C_i = \frac{M_i}{Q \times t} \quad (2)$$

The total mass concentration was calculated as follows:

$$C_{\text{total}} = \sum_{i=1}^{14} C_i \quad (3)$$

where Q and t are the sampling flow rate and time, respectively. Mass mean diameters (d_{MM}s) for fine (< 300 nm) and coarse (> 300 nm) modes were calculated using mass concentration from FP-XRF and ICP-MS as follows:

$$d_{MM} = \frac{\sum (C_i \times d_i)}{\sum C_i} \quad (4)$$

where d_i is the midpoint diameter at the i-th stage of the nano-MOUDI. Midpoint diameters and concentrations from 8th - 14th stages were used for fine mode, while midpoint diameters and concentrations from 1st - 7th stages were used for coarse mode.

The mass per substrate data produced by FP-XRF were compared to those from ICP-MS. The correlation between FP-XRF and ICP-MS was investigated using fitted linear regression models. The slope, y-intercept, and R^2 were calculated using Excel (14.0.7166.5000, Microsoft, USA).

2.3. Example Application: Estimation of Exposure and Dose

With the results from FP-XRF compared with ICP-MS, respiratory deposition of Fe and Cr particles was calculated from the respiratory deposition curve presented by ICRP (1994). Fractional mass concentrations calculated as follows:

$$C_X = \sum_{i=1}^{14} \left(C_i \times F_{X,i} \right) \quad (5)$$

where X represents the fraction (inhalable, Inh; respirable, Resp; particles deposited in the head airways, HA; particles deposited in the tracheobronchial, TB; and particles deposited in

the alveolar, AL). $F_{X,i}$ is the fraction for the i-th stage of the nano-MOUDI. These fractions were calculated using equations from Hinds (1999).

3. Results and Discussion

3.1. Development of a method to use FP-XRF with the nano-MOUDI

The original Al alloy holder and the custom PEEK substrate holders (both with and without the PC substrate) were analyzed for metals (Fe, Cr, Mn, Cu, Zn, Ni, Ti, and Pb) using FP-XRF (Table 1). Al was excluded because XRF detection is generally limited to elements with an atomic number greater than 16 (Brouwer, 2006) and because of the Al in the holder itself. Eight metals were detected in Al alloy holders with the magnet. Substantially fewer metals (Cr, Cu, and Ti) were measured in the PEEK holder and at lower concentrations than the Al alloy holders.

The presence of the PC substrate had no effect on the concentrations of metals measured in the Al or PEEK holders (Table 1). Hence, we conclude that neither the PC substrate nor oil on the substrate contained measureable metals. Moreover, these data provide evidence that the x-ray beam from the FP-XRF penetrates the substrate and excites metals in the holder.

Metals in blank MCE filters were measured by FP-XRF. The blank MCE filter was positioned in a thin-film holder instead of original filter holder. No metals were detected in blank MCE filters.

Metals (Fe and Cr) in blank PC substrates and MEC filters measured by ICP-MS are shown in Table 2. Less than 0.5 μg of Fe and Cr were detected in PC substrates and MEC filters. The limit of detection of ICP-MS can be calculated as the mean plus three standard deviations of the elemental mass per substrate found in blank substrates (IUPAC, 2006). However, the limit of detection of FP-XRF is difficult to calculate since the FP-XRF detected only Cr in PC blank substrate with PEEK holder while it detected no Fe in PC substrate with PEEK holder and no metals in MCE filters. The limit of detection for Cr could be calculated from M_{Ab} (Table1) and varied from 5.9 to 19.1 μg since the sampling area of nano-MOUDI stages varied from 1.77 to 5.73 cm^2.

3.2. Comparison of size distribution measurements analyzed by FP-XRF to ICP-MS

Particle size distributions measured by FP-XRF and the ICP-MS are shown in Figure 2. A bimodal distribution was observed with most particles in the fine mode and a small fraction of particles in a coarse mode. Whereas the fine mode was always visible for Fe and Cr when measured by FP-XRF and similar in magnitude to the ICP-MS, the second coarse mode was visible in only some of the size distributions measured with ICP-MS. The coarse mode was most prominent for Fe measured by ICP-MS. We believe that the coarse mode was visible only for ICP methods because ICP-MS can achieve limit of detections many orders of magnitude lower than FP-XRF with an instrumental limit of detection of 1-10 ppt. Therefore, the limit of detection of FP-XRF for Fe and Cr is expected to be higher than one for ICP-MS (Table 2). In fact for Cr, the calculated limit of detection of ICP-MS (0.14 μg) based on the blank substrate measurements were much smaller than one of FP-XRF (5.9 ~ 19.1 μg). Fe in blank substrates was detected only with ICP-MS. Therefore using the

instrumental limit of detection of the FP-XRF (standard 37-mm filter mode) for Fe and Cr were approximately 0.2 μg/cm^2 (Laohaudomchok et al., 2010) the method limit of detections by mass were estimated to be within 0.4 to 2.2 μg.

The mode diameters and total mass concentration are summarized in Table 3. Mode diameters for Fe and Cr obtained for the fine mode were similar between FP-XRF and ICP-MS. In contrast, coarse mode from FP-XRF were substantially smaller than those from ICP-MS. Fe and Cr collected on the substrates at the larger size stage in nano-MOUDI were detected more precisely by ICP-MS and this resulted in larger coarse mode diameter. Total mass concentrations for Fe and Cr from FP-XRF were similar to those from ICP-MS.

A scatter plot of mass detected on the substrate measured by FP-XRF relative to that from ICP-MS is shown in Figure 3. For both Fe and Cr, the mass detected by FP-XRF was linearly correlated with that measured by ICP-MS with most data near the 1:1 correlation line (illustrated by a dotted line). Fe was detected by both FP-XRF and ICP-MS at mass loadings higher than 2.5 μg but not by FP-XRF < 2.2 μg. Thus, at least 2.5 μg of Fe must be collected for detection by FP-XRF. Black dotted lines in Figure 2 identify these detectable Fe concentrations calculated from dividing 2.5 μg by actual sampling volumes. The detectable concentration was 1.0 μg/m^3 for the comparison of FP-XRF and ICP-MS. Using these computed detection limit, differences between results from FP-XRF and ICP-MS at the fine and coarse modes could be distinguished. Concentrations from FP-XRF, below the dotted line at the coarse mode, did not match well with the concentrations from ICP-MS.

The FP-XRF detected 30% more Cr than the ICP-MS as shown in Figure 3. One reason for these differences could be that experiments were conducted at the low concentrations near the detection limit of FP-XRF. Moreover, FP-XRF technique involved a single measurement location (at center of substrate), whereas ICP-MS measured all the particles collected on the substrate surface. Therefore, the one point measurement with FP-XRF at the low concentration may not accurately represent the total deposited mass averaged over the substrate surface.

Three data points (blue dot line in Figure 3) were far from the 1:1 line (black dot). Those points represent data collected on the MCE filters used in the last stage of the nano-MOUDI. The fact that particles are distributed over a much larger area on the MCE filter (10.75 cm^2) than the PC substrates (1.77 – 5.73 cm^2) increases uncertainty in the measurement of mass by FP-XRF. Also, uncertainty about the spatial distribution of particles on the MCE filter combined with the single FP-XRF measurement location (center) may have resulted in differences between analytical measurements. These error values from MCE filter could be multiplied when the mass per substrate is calculated using Equation 1.

3.3. Example application: Estimation of exposure and dose

One application of this method is to estimate the quantity of material deposited in human body. Concentrations of Fe and Cr particles deposited in the respiratory system are documented in Table 4. Total mass concentration measured by FP-XRF was the same as concentrations of inhalable and respirable particles because most test particles were smaller than 300 nm. When workers are exposed to 8.6 μg/m^3 of Fe and 4 μg/m^3 of Cr, the mass of

regional deposition can be predicted. Human inspiratory flow rate may vary from 0.39 to 3 m^3/h (Hinds, 1999). When an inspiratory volume was assumed to be 1.5 m^3 for one hour, total respirable depositions of Fe and Cr were is 13 μg and 6 μg, respectively. The estimated mass that would be collected in the alveolar region was 2.8 μg for Fe and 1.3 μg for Cr. A total of 22% of respirable Fe and Cr particles were estimated to be deposited in the alveolar region.

3.4. Limitations and recommendations

A limitation of this method is that at least one stage of the nano-MOUDI should collect more than 2.5 μg of Fe to distinguish a mode diameter. The threshold limit value (TLV) of Fe is 5000 μg/m^3 (ACGIH, 2006). If particles are sampled at a concentration of 10% of the TLVs for 10 minutes, the expected mass collected by the nano-MOUDI is 50 μg. If the mass fraction at the mode diameter is 20%, 10 μg of Fe could be collected on the substrate at a stage with a cutoff diameter similar to mode diameter. Thus, sampling for at 10 minutes is required with our method to distinguish mode diameter at a mass concentration of 1/10th TLV. Longer sampling time can allow for better correlation of FP-XRF and ICP-MS results. This study was also limited to fine-mode Fe and Cr particles. Future work will include testing coarse-mode and other metal-containing aerosol particles. The spark discharge system could be modified with different electrodes such as Mn, Cu, or Ti rods and the agglomeration chamber could be modified to increase the size of the test particles.

Removal of the magnet from the substrate holder did not affect uniformity of particle deposition. Uniform deposition was verified visually with new PEEK holders. Friction between the PEEK holder and the rotating plate was sufficient to keep the PEEK holder in place. However, care should be exercised to avoid tilting the nano-MOUDI and dislodging the holder from the rotating plate. Custom PEEK holders can be used for any kind of air sampling membrane filters with diameters of 47 mm.

4. Conclusion

We developed a rapid, on-site method to measure the metal content of aerosol particles, using a nano-MOUDI for particle collection across 14 size classes combined with a FP-XRF for non-destructive metals analysis. Custom substrate holders composed of PEEK enabled the direct measurement of nano-MOUDI substrates using FP-XRF. Results from FP-XRF compared favorably with those from ICP-MS. The shape of the size distributions produced by FP-XRF were similar to those obtained from ICP-MS. Results from FP-XRF were linearly correlated with results from ICP-MS ($R^2 = 0.91$ for Fe and $R^2 = 0.84$ for Cr). The mass of Fe detected by FP-XRF was similar to that detected by the ICP-MS for loadings greater than 2.5 μg per substrate. The proposed method can be used to rapidly measure the particle size distribution of metals..

Supplementary Material

Refer to Web version on PubMed Central for supplementary material.

Acknowledgments

References

ACGIH. Threshold Limit Values for Chemical Substances and Physical Agents & Biological Exposure Indices. ACGIH; Cincinnati, OH: 2014. American Conference of Governmental Industrial Hygienists.

Achad M, López ML, Ceppi S, Palancar GG, Tirao G, Toselli BM. Assessment of Fine and Sub-Micrometer Aerosols at an Urban Environment of Argentina. Atmos Environ. 2014; 92:522–532.

Ashley K. Field-Portable Methods for Monitoring Occupational Exposures to Metals. J Chem Health Safety. 2010; 17(3):22–28.

Broekaert JA, Wopenka B, Puxbaum H. Inductively Coupled Plasma Optical Emission Spectrometry for the Analysis of Aerosol Samples Collected by Cascade Impactors. Anal Chem. 1982; 54(13): 2174–2179.

Brouwer, P. Theory of XRF. Almelo, Netherlands: PANalytical BV; 2006.

Bukowiecki N, Hill M, Gehrig R, Zwicky CN, Lienemann P, Hegedüs F, Falkenberg G, Weingartner E, Baltensperger U. Trace Metals in Ambient Air: Hourly Size-Segregated Mass Concentrations Determined by Synchrotron-XRF. Environ Sci Tchnol. 2005; 39(15):5754–5762.

Chow JC, Watson JG. Review of Measurement Methods and Compositions for Ultrafine Particles. Aerosol Air Qual Res. 2007; 7(2):121–173.

Cuccia E, Massabò D, Ariola V, Bove MC, Fermo P, Piazzalunga A, Prati P. Size-Resolved Comprehensive Characterization of Airborne Particulate Matter. Atmos Environ. 2013; 67:14–26.

Espinosa AJF, Rodríguez MT, de la Rosa FJB, Sánchez JCJ. Size Distribution of Metals in Urban Aerosols in Seville (Spain). Atmos Environ. 2001; 35(14):2595–2601.

Espinosa AJF, Rodríguez MT, de la Rosa FJB, Sánchez JCJ. A Chemical Speciation of Trace Metals for Fine Urban Particles. Atmos Environ. 2002; 36(5):773–780.

Gorce JP, Roff M. Immediate Screening of Lead Exposure in the Workplace Using Portable X-Ray Fluorescence. J Occup Environ Hyg. 2016; 13(2):102–111. [PubMed: 26713915]

Harper M, Pacolay B, Hintz P, Bartley DL, Slaven JE, Andrew ME. Portable XRF Analysis of Occupational Air Filter Samples from Different Workplaces Using Different Samplers: Final Results, Summary and Conclusions. J Environ Monitor. 2007; 9(11):1263–1270.

Herner JD, Green PG, Kleeman MJ. Measuring the Trace Elemental Composition of Size-Resolved Airborne Particles. Environ Sci Technol. 2006; 40(6):1925–1933. [PubMed: 16570617]

Hering SV, Flagan RC, Friedlander SK. Design and Evaluation of New Low-Pressure Impactor. I Environ Sci Technol. 1978; 12(6):667–673.

Hinds, WC. Aerosol Technology: Properties, Behavior, and Measurement of Airborne Particles. 2nd ed.. NewYork: Wiley; 1999.

Hughes LS, Allen JO, Kleeman MJ, Johnson RJ, Cass GR, Gross DS, Gard EE, Gälli ME, Morrical BD, Fergenson DP, Dienes T. Size and Composition Distribution of Atmospheric Particles in Southern California. Environ Sci Technol. 1999; 33(20):3506–3515.

ICRP. Human Respiratory Tract Model for Radiological Protection. Elsevier Science, Ltd.; Oxford, U.K.: 1994. International Commission on Radiological Protection. Publication 66

McNaught, AD., Wilkinson, A., editors; Nic, M.Jirat, J., Kosata, B., editors. IUPAC. Compendium of Chemical Terminology. 2006. (Series Eds.)*the "Gold Book"* Retrieved from http://www.iupac.org/goldbook/L03540.pdf

Laohaudomchok W, Cavallari JM, Fang SC, Lin X, Herrick RF, Christiani DC, Weisskopf MG. Assessment of Occupational Exposure to Manganese and Other Metals in Welding Fumes by Portable X-Ray Fluorescence Spectrometer. J Occup Environ Hyg. 2010; 7(8):456–465. [PubMed: 20526948]

Marple VA, Rubow KL, Behm SM. A Microorifice Uniform Deposit Impactor (MOUDI): Description, Calibration, and Use. Aerosol Sci Technol. 1991; 14(4):434–446.

Marple V, Olson B, Romay F, Hudak G, Geerts SM, Lundgren D. Second Generation Micro-Orifice Uniform Deposit Impactor, 120 MOUDI-II: Design, Evaluation, and Application to Long-Term Ambient Sampling. Aerosol Sci Technol. 2014; 48(4):427–433.

Mudunkotuwa IA, Anthony TR, Grassian VH, Peters TM. Accurate Quantification of TiO_2 Nanoparticles Collected on Air Filters Using a Microwave-Assisted Acid Digestion Method. J Occup Environ Hyg. 2016; 13(1):30–39. [PubMed: 26181824]

NIOSH. National Institute for Occupational Safety and Health. NIOSH Manual of Analytical Methods. 4. Method 7702 Lead by Field Portable XRF. 1998 DHHS (NIOSH) Publication No. 98-119.

Onat B, ahin ÜA, Bayat C. Assessment of Particulate Matter in the Urban Atmosphere: Size Distribution, Metal Composition and Source Characterization Using Principal Component Analysis. J Environ Monitor. 2012; 14(5):1400–1409.

Park JH, Mudunkotuwa IA, Mines LW, Anthony TR, Grassian VH, Peters TM. A Granular Bed for Use in a Nanoparticle Respiratory Deposition Sampler. Aerosol Sci Technol. 2015; 49(3):179–187. [PubMed: 26900208]
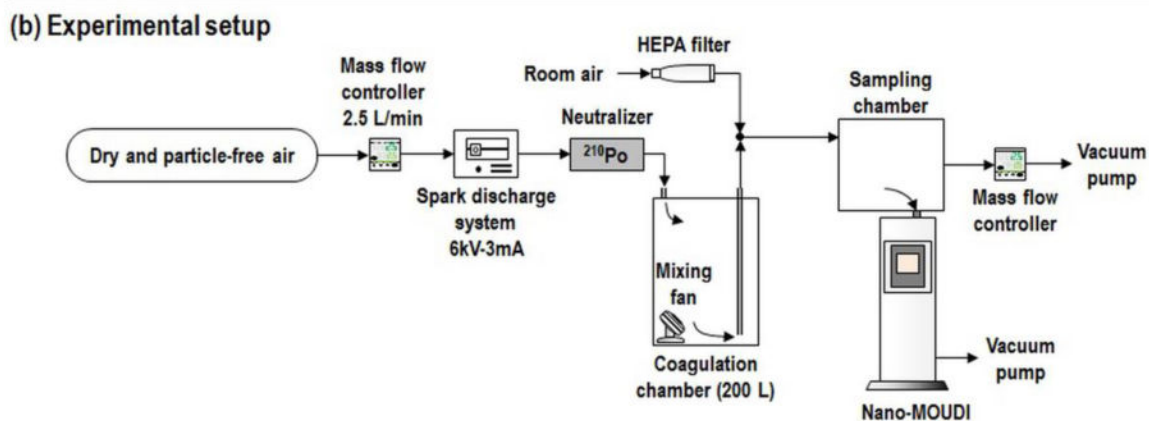
Fig. 1.
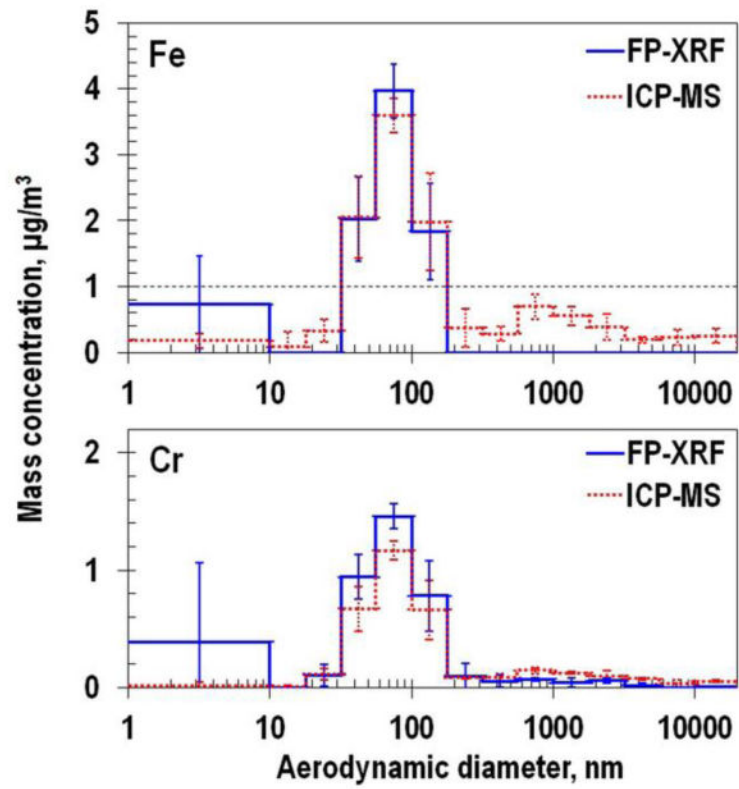(a) FP-XRF setup and (b) experimental setup.

Fig. 2.
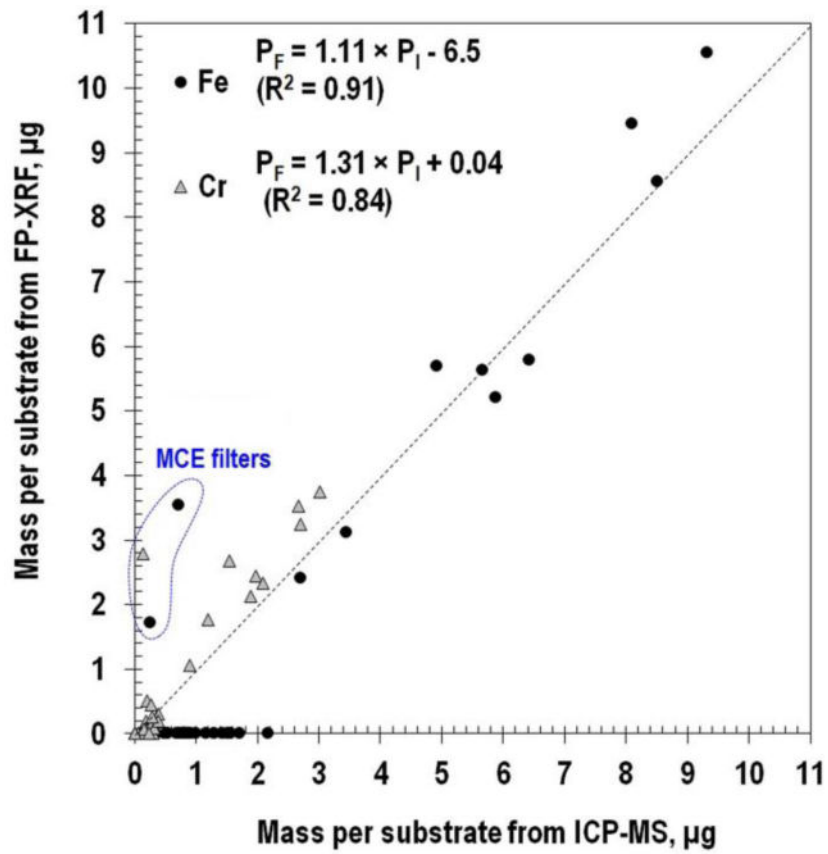Results for size distribution of Fe and Cr from FP-XRF and ICP-MS.

Fig. 3.
Mass per substrate from FP-XRF and ICP-MS.

Table 1

Summary of results for metals in substrate holders analyzed by FP-XRF (mean ± standard deviation of three measurements, N.D.: not detected, N: number of measurements)

Metal	[a]Al alloy holder, μg/cm²		[b]PEEK holder, μg/cm²	
	w/o PC substrate (N = 3)	w/ PC substrate (N = 9)	w/o PC substrate (N = 3)	w/ PC substrate (N = 9)
Fe	24.8 ± 0.5	28.2 ± 6.9	N.D.	N.D.
Cr	4.6 ± 0.1	4.6 ± 0.2	3.2 ± 0.1	3.2 ± 0.1
Mn	6.2 ± 0.5	5.7 ± 0.9	N.D.	N.D.
Cu	57.1 ± 0.6	56.5 ± 1.2	1.6 ± 0.1	1.7 ± 0.1
Zn	14.6 ± 0.1	15.3 ± 1.3	N.D.	N.D.
Ni	73.5 ± 19.7	71.7 ± 14.2	N.D.	N.D.
Ti	1.3 ± 0.0	1.3 ± 0.1	0.6 ± 0.1	0.6 ± 0.1
Pb	2.0 ± 0.1	3.1 ± 2.3	N.D.	N.D.

[a]Al alloy holder supplied by the company,

[b]custom made holder, PC: polycarbonate

Table 2

Background metals content in blank substrates.

Blank	Metal	[a]μg per substrate	[b]Limit of detection, μg
PC substrate	Fe	0.49 ± 0.19	1.06
	Cr	0.08 ± 0.02	0.14
MCE filter	Fe	0.09 ± 0.05	0.24
	Cr	0.13 ± 0.03	0.21

[a] measured by ICP-MS, mean ± standard deviation,

[b] mean plus three standard deviations

Table 3

Summary of particle characteristics calculated using the results from FP-XRF and ICP-MS

Method	Metal	[a]Mode diameter, nm	Mass mean diameter for fine mode, nm	Mass mean diameter for coarse mode, nm	[b]Total mass concentration, µg/m³
FP-XRF	Fe	78	77	-	8.6 ± 2.0
	Cr	78, 780	78	1699	4.0 ± 1.0
ICP-MS	Fe	78, 780	88	3392	11.2 ± 2.0
	Cr	78, 780	87	3204	3.3 ± 0.5

[a]
two diameters for bimodal distribution,

[b]
mean ± standard deviation of three measurements

Table 4

Estimated concentrations of inhalable, respirable particles, and regional deposited particles, using FP-XRF analysis.

Metal	Total mass concentration, µg/m³	Inhalable, µg/m³	Respirable, µg/m³	Head airways, µg/m³	Tracheobronchial region, µg/m³	Alveolar region, µg/m³
Fe	12.8	12.8	12.8	0.7	0.8	2.8
Cr	6.0	6.0	6.0	0.5	0.4	1.3